Physics Letters B 843 (2023) 138058

Contents lists available at ScienceDirect

Physics Letters B

journal homepage: www.elsevier.com/locate/physletb

High precision fundamental physics experiments using compact spin-transparent storage rings of low energy polarized electron beams

Riad Suleiman [a,*], Vasiliy S. Morozov [b], Yaroslav S. Derbenev [a]

[a] Thomas Jefferson National Accelerator Facility, Newport News, 23606, VA, USA
[b] Oak Ridge National Laboratory, Oak Ridge, 37831, TN, USA

ARTICLE INFO

Article history:
Received 16 May 2023
Received in revised form 14 June 2023
Accepted 28 June 2023
Available online 3 July 2023
Editor: D.F. Geesaman

Keywords:
Electron electric dipole moment
CP violation
Dark matter and dark energy
Polarized electron beam
Spin-transparent storage ring

ABSTRACT

We present a new design of highly specialized small storage rings for low energy polarized electron beams. The new design is based on the transparent spin methodology that cancels the spin precession due to the magnetic dipole moment at any energy while allowing for spin precession induced by the fundamental physics of interest to accumulate. The buildup of the vertical component of beam polarization can be measured using standard Mott polarimetry that is optimal at low electron energy. Systematic effects are suppressed using counter-rotating bunched beams with various polarization orientations. These rings can be used to directly measure the permanent electric dipole moment of the electron, relevant to CP violation and matter-antimatter asymmetry in the universe, and to search for dark energy and ultra-light dark matter.

1. Introduction

The electric dipole moment (EDM) is very sensitive to physics beyond the Standard Model and new sources of Charge-conjugation and Parity (CP) violation [1–3]. Such CP violation, beyond what is present in the weak interaction, could signal the presence of new physics and explain the puzzle of the matter-antimatter asymmetry in the universe. However, there are no direct measurements of the electron or proton EDMs. The EDM upper limit of the electron ($d_e < 4.1 \times 10^{-30}$ e · cm, 90% C.L.) has been extracted from a measurement using HfF^+ ion [4] while the proton limit was obtained using ^{199}Hg atom [5]. Direct measurements of the EDM upper limits only exist for the neutron [6] and the muon [7] where the muon limit was measured in conjunction with the anomalous magnetic dipole moment, $g-2(\equiv 2G)$.

Any measurement of EDM relies on measuring the spin precession rate in an electric field of a particle's rest frame, $\frac{d\vec{S}}{d\tau} = \vec{\mu} \times \vec{B}_{\text{rest}} + \vec{d} \times \vec{E}_{\text{rest}}$, where the magnetic dipole moment (MDM) and EDM are defined as $\vec{\mu} = (G+1)\frac{q}{mc}\vec{S}$ and $\vec{d} = \frac{\eta}{2}\frac{q}{mc}\vec{S}$, q and m are the particle charge and mass, c is the speed of light, η is the electric dipole factor, and $\vec{S}$ represents spin in the particle's rest frame. However, since an electric field leads to acceleration for charged particles, such measurement cannot be made while keeping the particle at rest. Therefore, to both apply an electric field and trap a charged particle, a storage ring must be used. For a charged particle moving in transverse ($\vec{E}_\perp$) and longitudinal ($\vec{E}_\parallel$) electric and magnetic ($\vec{B}$) fields given in the lab frame, the generalized Thomas-BMT equation of spin precession is $\frac{d\vec{S}}{dt} = (\vec{\omega}_{\text{MDM}} + \vec{\omega}_{\text{EDM}}) \times \vec{S}$ with [8]:

$$\vec{\omega}_{\text{EDM}} = -\frac{\eta q}{2mc}\left(\frac{1}{\gamma}\vec{E}_\parallel + \vec{E}_\perp + \vec{\beta} \times \vec{B}\right), \tag{1}$$

where $\vec{v} \equiv \vec{\beta}c$ and γ are the particle's velocity and Lorentz energy factor.

The basic principle of the EDM measurement in a ring relies on making MDM spin rotation effectively vanish. Observation of a spin rotation then indicates the presence of EDM. Strategies to cancel MDM spin precession can be formulated for particle motion along a closed reference design orbit, traditionally (but not necessarily) in a plane, that permit the effective stacking of the EDM precession turn by turn around the orbit. A flat reference orbit generally employs vertical magnetic (B_y) and horizontal transverse electric (E_x) fields. In the accelerator reference frame, spin then precesses due to MDM about vertical axis with angular frequency, ω_y:

$$\omega_{y,\text{MDM}} = -\frac{q}{mc}\left(GB_y - \frac{1-\gamma^2\beta^2 G}{\gamma^2\beta}E_x\right). \tag{2}$$

Considering Eq. (2), two experimental approaches have been developed to compensate MDM spin rotation and thereby measure EDM in storage rings:

* Corresponding author.
E-mail address: suleiman@jlab.org (R. Suleiman).

https://doi.org/10.1016/j.physletb.2023.138058

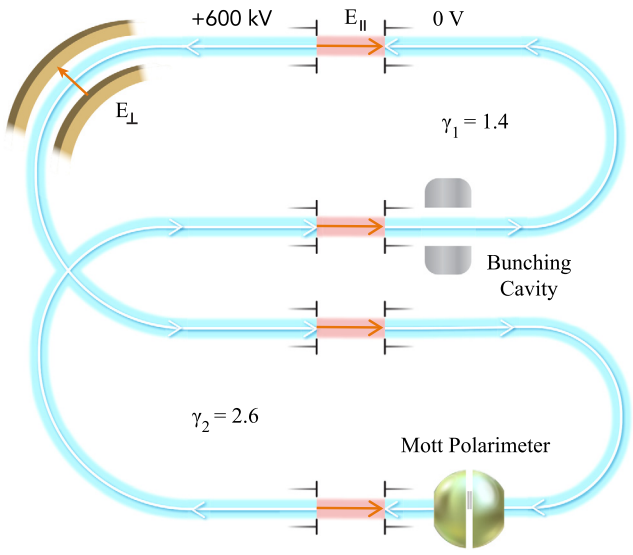

Fig. 1. Layout of a two-energy ST storage ring for measuring the electron EDM (figure not drawn to scale). Only one of the two CR electron beams is shown. The ring uses only static electric fields ($E_\parallel$ and $E_\perp$) except for a single RF bunching cavity. The high-energy arcs are floating at high voltage of 600 kV. Both vertical and horizontal polarization components can be simultaneously measured using a Mott polarimeter.

1. All-electric ring with $B_y = 0$ and $\gamma^2 = 1 + 1/G$, described as the magic energy (ME) approach [9]. This works only for $G > 0$ (e.g., electron or proton) and at a very specific energy. Two experiments have been proposed to measure the proton EDM (d_p) with a sensitivity of 10^{-29} $e \cdot$cm at ME of 232.8 MeV in rings with ≥ 500 m circumference [10–14].
2. Combined electric/magnetic ring with $GB_y = (1 - \gamma^2\beta^2 G)/(\gamma^2\beta)E_x$. An experiment is planned to measure the deuteron ($G = -0.143$) EDM (d_d) at 1.0 GeV/c with such a ring [15].

Notably, these experiments propose to measure d_p and d_d but not d_e. In fact, there is no d_e proposal at ME ($\gamma = 29.38$, 15.01 MeV) because there is no viable polarimetry at this electron beam energy.

This paper briefly presents a method to measure d_e in a small storage rings with beam energy below 1 MeV. More details can be found in Ref. [16]. It is based on the Figure-8 spin-transparent (ST) configuration [17,18] where the MDM signal is naturally suppressed at any energy due to the ring topology and symmetry. Thus, there is no spin decoherence due to the beam energy spread. To reduce systematic effects, we consider an all-electric design with no magnetic fields to allow for two counter-rotating (CR) electron beams A and B (CRA and CRB) to circulate concurrently.

For EDM searches, the challenge consists of accounting for all systematic effects associated with field errors, beam emittances, and background magnetic fields that could mimic the EDM signal, and compensating for them. For example, one must eliminate the MDM spin effect due to closed orbit excursion and beam emittances. Closed orbit excursion is always present in a real ring. Techniques have already been developed for compensating the first and second order effects of imperfections on the spin in ST rings. They have been verified by simulations while designing polarized beams in Figure-8 rings for the Jefferson Lab Electron-Ion Collider [17]. The small-scale size of the proposed ring greatly simplifies the problem of error control.

2. EDM spin-transparent ring concept

The EDM ST ring illustrated in Fig. 1 consists of two low-energy and two high-energy arcs connected by longitudinal static electric field sections to provide acceleration/deceleration. They preserve suppression of the MDM effect but remove the degeneracy of the EDM spin precession. The beam directions in the two arcs of each energy are opposite making the net bending angle zero. A straightforward way to obtain the EDM spin rotation per turn N around the ring, $\partial\,|\psi_\mathrm{EDM}|\,/\partial N$, is to treat the EDM signal as a perturbation of the MDM spin motion on the closed orbit [17]. Equation (1) can be readily used to find:

$$\frac{\partial\,|\psi_\mathrm{EDM}|}{\partial N} = \left| 2\eta \left[\frac{\gamma_2^2\beta_2}{1-\gamma_2^2\beta_2^2 G} - \frac{\gamma_1^2\beta_1}{1-\gamma_1^2\beta_1^2 G} - \ln\frac{\gamma_2+\sqrt{\gamma_2^2-1}}{\gamma_1+\sqrt{\gamma_1^2-1}} \right] \sin\left(\frac{\omega_M^1}{2}\pi\right) \sin\left(\frac{\omega_M^2}{2}\pi\right) \right|, \tag{3}$$

with the spin rotation axis lying in the horizontal plane. A detailed derivation of Eq. (3) can be found in Ref. [16]. The quantity ω_M^n in Eq. (3) is the spin precession due to MDM per unit orbital angle in transverse electric field given by $\omega_M^n \equiv -(1 + G - \gamma_n^2 G)/\gamma_n$, where $n = 1, 2$ specifies γ_n in the two different energy regions.

The EDM spin rotation per unit η and unit time is $\Omega_\mathrm{EDM} \equiv \partial^2\,|\psi_\mathrm{EDM}|/\partial\eta\partial t = f_c\,\partial^2\,|\psi_\mathrm{EDM}|/\partial\eta\partial N$ where f_c is the beam circulation frequency. Fig. 2 shows Ω_EDM as a function of γ_1 and γ_2 where we assumed bending and accelerating/decelerating electric fields of $|E| = 10$ MV/m and a packing factor of 0.5 (conceptual design scenario). Fig. 2 indicates that reaching a substantial EDM signal requires a significant difference between γ_1 and γ_2. As an example, for $\gamma_1 = 1.4$ and $\gamma_2 = 2.6$, corresponding to 200 keV beam from the electron source and the high-energy arcs floating at high voltage of 600 kV, $\Omega_\mathrm{EDM} = 0.46 \times 10^9$ rad/s.

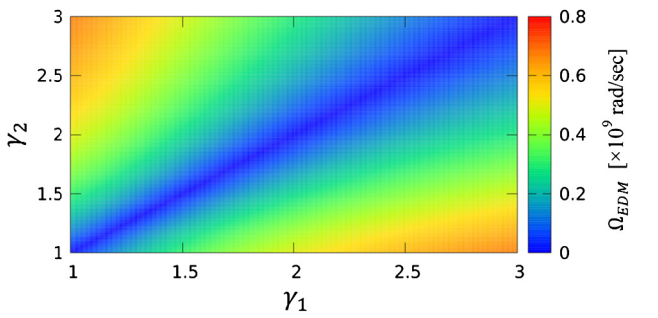

Fig. 2. Magnitude of the EDM spin rotation per unit η per unit time Ω_EDM as a function of γ_1 and γ_2 for the conceptual scenario.

For the ME racetrack approach, EDM spin precession per turn is $\Omega_\mathrm{EDM} = \pi/\sqrt{G}$. Under the same field and packing factor assumptions as above, $\Omega_\mathrm{EDM} = 1.47 \times 10^9$ rad/s. Thus, the above conceptual consideration provides an EDM spin rotation achievable in an ST ring that is only a factor of 3 smaller than that of an ME ring but with vastly smaller footprint, and other advantages. The particular ST ring design described below (and shown in Fig. 4) accounts for practical aspects and results in $\Omega_\mathrm{EDM} = 0.29 \times 10^9$ rad/s, which is somewhat lower than in the conceptual case but is still in a reasonable agreement with it. The results of the ST and ME rings comparison are summarized in Table 1.

Assuming $\eta = 6.0 \times 10^{-19}$ (see Section 7), the expected EDM spin precession rate in the ST ring of Fig. 4 is $\partial\,|\psi_\mathrm{EDM}|/\partial t = \Omega_\mathrm{EDM} \times \eta = 0.17$ nrad/s. This rate is experimentally discernible given adequate suppression of systematic effects.

3. Optics design

Searching for an EDM signal requires detection of minute changes in the beam's polarization. Therefore, the polarimeter

Table 1
Comparison of EDM spin rotations in the ME and ST rings.

Approach	γ	$\left\|\frac{\partial^2 \|\psi_{EDM}\|}{\partial\eta\partial N}\right\|$ (rad)	Ω_{EDM} ($\times 10^9$ rad/s)
ME	29.38	92.24	1.47
ST (conceptual)	(1.4, 2.6)	4.24	0.46
ST (of Fig. 4)	(1.4, 2.6)	4.24	0.29

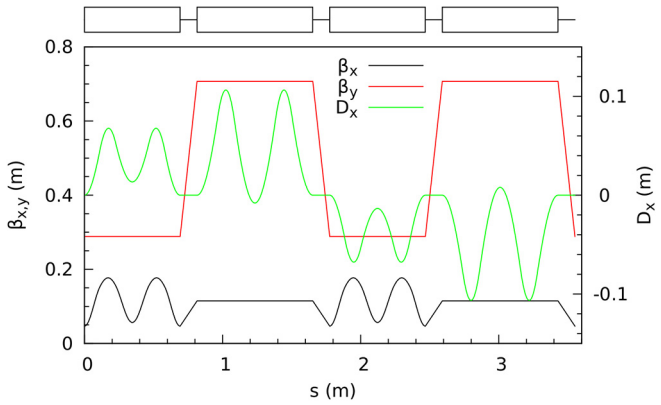

Fig. 3. Optics of the entire EDM ST ring showing the Twiss β functions in both planes ($\beta_{x,y}$) and the horizontal dispersion (D_x) along the ring.

must provide high-precision measurement of the polarization during an experiment. With systematic effects suppressed as discussed in Section 8, the measurement precision is determined by the statistical error. Thus, one must store a sufficiently large number of particles in the ring. The statistical considerations for the polarimetry suggest the following procedure. Four bunches, each with 2 nC electron charge, are initially injected in each direction of circulation. The initial beam polarization is then immediately measured with good statistics reducing the bunch charge down to 1 nC ($N_e = 6.24 \times 10^9$ of stored electrons). The reduced-charge bunches are stored for an extended period of time and their polarization is monitored for an EDM signal. The resulting statistics provides an adequate sensitivity level as discussed below.

3.1. Transverse dynamics

For the optical structure of the arcs of the ST ring, we recommend the design described in Ref. [19] which employs weak-focusing optics. The horizontal focusing is set by the orbit bend radius, while the vertical one is provided by a weak vertical-focusing gradient of the electric field. The dispersion is controlled by changing the bending direction. The main drawback of this design is that the reverse bends do not contribute to the out-of-plane rotation of the EDM signal. However, this disadvantage is offset by a high packing factor compared to other designs.

We assume longitudinal fields of 5 MV/m and bending fields of ≤ 10 MV/m on the design orbit. Small beam sizes are required to have sufficient beam aperture and to maintain long beam lifetime. Fig. 3 shows the resulting optics of the entire ring. The corresponding footprint of the ring is shown in Fig. 4 and the main parameters of the ring design are summarized in Table 2.

3.2. Longitudinal dynamics

Beam bunching is necessary to distinguish and stochastically cool simultaneously-stored CR electron beams and as a means of efficient suppression of systematic effects. Therefore, a bunching RF cavity is inserted into the ring. In a matched equilibrium state with weak longitudinal focusing, each bunch has nearly constant length

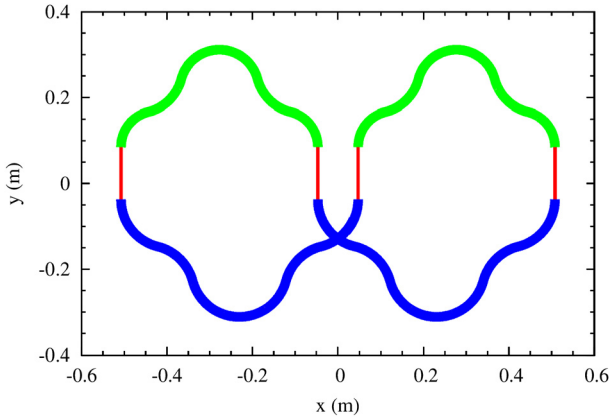

Fig. 4. Footprint of the EDM ST ring drawn to scale showing the high-energy arcs in blue, the low-energy arcs in green, and the longitudinal static electric field sections in red.

Table 2
EDM ST ring and beam parameters.

Quantity	Value
γ_1, γ_2	1.4, 2.6
Ring circumference	3.55 m
Circulation frequency f_c	68.5 MHz
Straight section length	12.3 cm
Beam pipe aperture	± 3 cm
Longitudinal field $\|E_\parallel\|$	5 MV/m
Arc bending fields $\|E_\perp\|$	3.3 – 10 MV/m
Number of bunches	4 CRA and 4 CRB
Charge per bunch	2 nC at injection, 1 nC at store
Beam current	274 mA CRA and CRB

Table 3
Longitudinal dynamics parameters for a stochastically cooled beam. The bunching cavity is placed in the low-energy section.

Quantity	Value
Harmonic number	5
RF frequency	342.6 MHz
Bunch length	17.8 cm
Bunching voltage amplitude	1.67 kV
Synchrotron tune	0.029

and root-mean-square (rms) absolute momentum spread around the ring.

We choose a harmonic number of five providing sufficient bucket length for relatively intense bunches. Four of the buckets are filled while the fifth one is kept empty for the purposes of injection, extraction and ion cloud clearing. Considering densely populated buckets, we assume one quarter of the bucket length to be the rms bunch length. The equilibrium momentum spread at that bunch length is determined by a balance of the intra-beam scattering (IBS) diffusion and stochastic cooling as discussed in Section 4. For a cooled bunched beam with the bunching cavity placed in the low-energy section, the voltage required is given in Table 3 along with other key parameters relevant to the longitudinal beam dynamics in the two-energy ring.

4. Beam physics issues and limitations

Measuring d_e to 10^{-30} $e \cdot$cm level requires a relatively high stored charge of 1 nC in each bunch. In combination with our choice of low beam energies, IBS will cause large beam sizes. We use the optics shown in Fig. 3 and the ring parameters listed in Table 2 to estimate the emittance limitations imposed by IBS. We find transverse emittances and momentum spread [20,21] that give

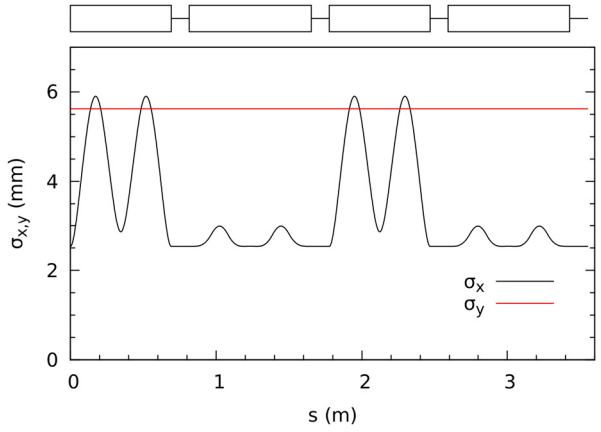

Fig. 5. Beam sizes along the EDM ring when stochastic cooling is applied.

equal IBS growth times $\tau^{\rm IBS}_{x/y/z}$ of 10^4 s in the three dimensions. This corresponds to a fairly large maximum rms horizontal/vertical beam size of $\sigma_x/\sigma_y = 25/19$ mm.

To reduce beam sizes, we must apply stochastic cooling. A typical time of stochastic cooling, assuming the number of electrons N_e of 6.24×10^9 and the cooling system's bandwidth W of 10 GHz [22–24], is $\tau^{\rm cool}_z \sim \frac{N_e}{2W} \sim 0.3$ s. We conservatively use a longitudinal cooling time $\tau^{\rm cool}_z$ of 4 s. We assume that cooling is primarily longitudinal with 10% of the total cooling decrement coupled into the transverse dimensions. Since the IBS rates are determined by the equilibrium with the cooling rates, we find transverse emittances and momentum spread resulting in $\tau^{\rm IBS}_x = \tau^{\rm IBS}_y = 40$ s and $\tau^{\rm IBS}_z = 4$ s. With stochastic cooling, the beam sizes are shown in Fig. 5, which are manageable.

Another potential limitation on the amount of stored charge comes from the betatron tune shifts $\Delta\nu^{\rm SC}_{x/y}$ due to space charge fields. Beam stability requires that $|\Delta\nu^{\rm SC}_{x/y}|$ do not exceed the space charge threshold $|\Delta\nu^{\rm thr}_{x/y}|$ of about 0.3 (or even higher [25,26]). Using the cooled beam parameters, the direct space-charge tune shift is $\Delta\nu^{\rm SC}_{x/y} = 3.4/4.2 \times 10^{-2}$. More importantly, each stored beam experiences the field of the CR beam. Its local effect is a factor of $\gamma^2(1+\beta^2)$ stronger than the self-field interaction. The resulting tune shift is a factor of about 6 greater than that of a single beam. Fortunately, it is still consistent with the typical threshold of 0.3.

We also investigated issues related to microwave instabilities of our low-energy electron beams. At these energies, the Coulomb intra-beam and CR beams interactions are dominant compared with influence of the external and radiation impedances. However, strong Landau damping due to the large energy spread at equilibrium prevents development of the Coulomb instabilities.

For electrons with $\gamma = 2.6$, the power radiated by a single electron in free-space is estimated to be about 0.3 keV/s and for $\gamma = 29.38$ (the ME case) the synchrotron radiation is about 35 keV/s per single electron. For the new ST ring described here, at this low electron energy combined with the proposed vacuum chamber design, some shielding effect is expected that suppresses the emission of synchrotron radiation [27,28] such that the bunching cavity can easily compensate for this energy loss. In contrast, there is no such shielding effect in the magic energy ring and synchrotron radiation is another major drawback when compared to the low energy ST ring.

Beam lifetime should be at least as long as the spin coherence time (SCT). As discussed above, stochastic cooling can overcome the IBS effect. Thus, the beam lifetime will be limited by other mechanisms. The vacuum level in such a small ring can be as low as 1×10^{-12} Torr (dominated by H_2 molecules) [29] and residual gas scattering will not be a limiting factor. The total energy loss per electron due to interaction with residual gas molecules after 1 day of store time is estimated to be 1.1 keV and, as in the case of synchrotron radiation, the bunching cavity will compensate for any energy loss. The expected lifetime due to the CR beam-beam interaction is estimated to be more than 1 day. No energy loss is expected here since the identical beams are moving in opposite directions, *i.e.*, no energy exchange in the scattering but the emittance is affected because of the angular distribution.

5. Spin stability and precision control

SCT is the time beam stays polarized in the storage ring. It is important to have a long SCT since this is the time available to accumulate and observe the EDM signal. After beam has been stored one unit of SCT, the second beam polarization measurement is performed. For the second polarization measurement, the second half of the beam is extracted on the polarimeter target. The proton EDM proposals at magic energy are limited by SCT of about 1000 s [15], where depolarization is caused by the spread in MDM spin precession mainly due to energy spread and being slightly off exact magic energy, while the beam lifetime is much longer. Since in our case the spin tune is energy independent, the energy spread does not contribute to depolarization in the first order. The main limitation comes from the spin tune spread due to the beam emittances.

The spin motion in an ST ring is governed by a zero-integer spin resonance. The main parameter describing a spin resonance is its strength defined as the number of spin precessions per unit turn. The zero-integer spin resonance strength consists of coherent and incoherent parts. The coherent part is determined by the ring imperfections and is the same for all particles. Thus, it does not cause depolarization. It can be precisely compensated using weak correcting elements and its residual effects can be further suppressed by comparing polarization dynamics of the CR beams. The limit on SCT is determined primarily by the incoherent part of the spin resonance ε_{inc}, which causes the spins of particles with different betatron and synchrotron amplitudes to precess at slightly different rates. There are also other effects, such as spin diffusion due to stochastic cooling, that need further study.

The ST theory [30] still needs to be extended to electric rings to provide an analytic expectation for ε_{inc} in the proposed ring described above. For now, we only provide an upper limit on ε_{inc} based on the desired coherence time τ_{coh}. Consider a particle with its motion invariants equal to the rms emittances of the bunch. Let us define τ_{coh} as the amount of time it takes the spin of such a particle to deviate by 60° from its original direction. The spin component of this particle along the initial spin direction is then equal to $\cos 60^\circ = 1/2$ of its original value. Since the number of turns it takes the spin to complete such a rotation is $N_{coh} = 1/(6\varepsilon_{inc})$, ε_{inc} must satisfy

$$\varepsilon_{inc} < \frac{1}{6\tau_{coh} f_c}. \tag{4}$$

For τ_{coh} of 10^5 s (about 1 day) and f_c of Table 2, Eq. (4) gives $\varepsilon_{inc} < 2.4 \cdot 10^{-14}$. Just for scale, such levels of ε_{inc} are reachable in magnetic ST rings even without applying any special suppression measures [31].

6. Polarized electron source and Mott polarimeter

Nowadays, polarized electron sources can deliver beam polarization of 0.90 on a regular basis. Details about a polarized electron source can be found in Refs. [32–34].

The build-up of the vertical component of the electron beam polarization due to spin precession from longitudinal to vertical

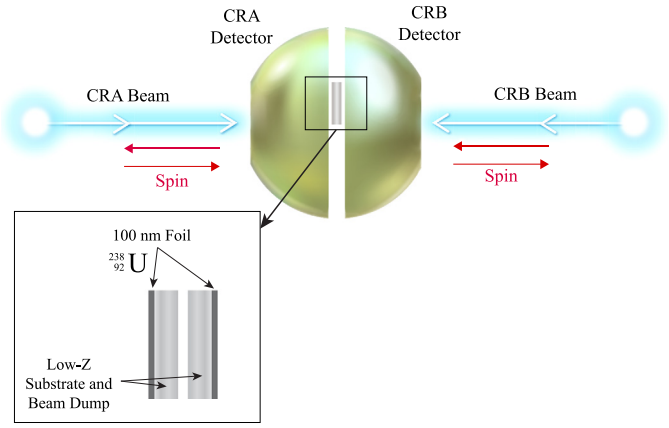

Fig. 6. Schematic of the Mott polarimeter.

caused by EDM can be measured using a conventional Mott polarimeter [35–38]. The polarimeter can simultaneously determine both the horizontal and vertical asymmetries. The horizontal asymmetry is sensitive to the vertical polarization component and thus the physics of interest while the vertical asymmetry will be used to monitor the horizontal polarization component. For 200 keV kinetic energy electrons scattered from ^{238}U [39,40], the analyzing power of Mott scattering from a single atom can be as large as 0.56 at scattering angle of 130°.

A schematic of a Mott polarimeter is shown in Fig. 6. The target is made of two 100 nm ^{238}U foils with a low-Z substrate as a beam dump. The detectors cover the scattering angles from 90° to 160° with full azimuthal coverage. For this design, the polarimeter efficiency (ϵ) is 0.0024 and the average analyzing power (A_y) is 0.45.

7. Expected electron EDM statistical limit

One possible scheme to operate the EDM ST storage ring and perform Mott measurements is as follows:

- Ring is filled with four polarized electron bunches, each 2 nC, in one direction and another four bunches, each 2 nC, in opposite direction.
- Four possible filling schemes for CRA:
  1. First bunch with positive helicity (CRA,+h), second bunch with negative helicity (CRA,-h), or
  2. First bunch with negative helicity (CRA,-h), second bunch with positive helicity (CRA,+h).
  3. Third bunch with in-radial polarization (CRA,+r), fourth bunch with out-radial polarization (CRA,-r), or
  4. Third bunch with out-radial polarization (CRA,-r), fourth bunch with in-radial polarization (CRA,+r). Or,
  5. Third bunch with up-vertical polarization (CRA,+v), fourth bunch with down-vertical polarization (CRA,-v), or
  6. Third bunch with down-vertical polarization (CRA,-v), fourth bunch with up-vertical polarization (CRA,+v).
- Four possible filling schemes for CRB - similar to CRA.
- Use half the charge of each bunch to measure the initial bunch polarization at $t = 0$. Now, each bunch is 1 nC.
- Store for period of SCT = 1 day.
- The longitudinally polarized bunches will be used to measure EDM while the radial and vertical polarized bunches will be used to measure the systematic uncertainties related to background electromagnetic fields.
- EDM will accumulate a positive vertical polarization component for (CRA,+h) and (CRB,-h) and negative vertical component for (CRA,-h) and (CRB,+h).

Table 4
Parameters used to evaluate the statistical uncertainty of the EDM measurement.

Spin quantum number	s	$\frac{1}{2}$
Electrons per fill	N_e	5.0×10^{10}
Longitudinal polarization	P	0.90
Polarimeter efficiency	ϵ	0.0024
Analyzing power	A_y	0.45
Spin rotation per η per time	Ω_{EDM}	0.29×10^{9} rad/s
Spin coherence time	SCT	1 day (86400 s)

- Measure left-right and up-down asymmetries at the end of store time, $t =$ SCT by having the bunches intercept the Mott target.
- Measure scattered electron asymmetries of each beam in its back-angle detector. Forward scattered electrons will be stopped in the substrate. Target ladder will be electrically isolated to measure intercepted charge from each bunch.
- Mott measurement statistical uncertainty of vertical polarization due to EDM spin precession per fill (CRA and CRB) is $\delta P \approx 0.020\%$.
- After total running of 1825 fills (or five years), achieve measurement of vertical polarization due to EDM spin precession to statistical uncertainty of $\delta P \approx 4.7 \times 10^{-6}$ or 4.7 μ rad.

For this polarization measurement scheme, the statistical uncertainty of the EDM measurement per fill can be calculated as [11,41]:

$$\sigma_{\mathrm{EDM}} = \sqrt{8}\frac{qs\hbar}{2mc}\frac{1}{\sqrt{N_e\,\epsilon}\;A_y\;P\;\Omega_{\mathrm{EDM}}\;\mathrm{SCT}}\,. \tag{5}$$

With the numerical values given in Table 4, $\sigma_{\mathrm{EDM}} = 2.5 \times 10^{-28}\ e \cdot \mathrm{cm}$. After five years of data taking, the projected statistical limit is about $5.8 \times 10^{-30}\ e \cdot \mathrm{cm}$ (corresponding to $\eta = 6.0 \times 10^{-19}$) with the expectation that further optimization and improvements will lower this limit.

8. Systematic effects

Since the spin rotation due to EDM is much smaller than that of the MDM ($\eta/G \approx 10^{-15}$), uncontrolled MDM spin rotations limit the smallest EDM that can be measured and introduce systematic uncertainties [14,42]. In the ST ring, MDM spin rotations should average to zero over a single turn, however, fringe and background electromagnetic fields and errors in the construction and alignment of the ring elements may introduce non-zero MDM spin rotations. One approach to further suppress residual MDM effects is the use of state-of-the-art shielding of background fields where the small size of the ST ring makes elaborate shielding very practical. Another approach relies on the fact that EDM is time-reversal violating while the majority of the experimental systematic effects are time-reversal conserving. The time-reversal is implemented by the use of CR beams. A third approach is to rely on the electron helicity ($\pm$h) reversal and combine data collected during EDM measurements as: $((\mathrm{CRA}, +\mathrm{h}) - (\mathrm{CRA}, -\mathrm{h}) + (\mathrm{CRB}, -\mathrm{h}) - (\mathrm{CRB}, +\mathrm{h}))/4$. Finally, a fourth approach will use two of the four bunches (with either radial or vertical polarization, as was discussed in the previous section) in each direction of the ring to control background electromagnetic fields. Not all systematic effects cancel with either beam velocity or spin reversals, some systematic effects (e.g., a radial background magnetic field that generates a vertical spin rotation identical to EDM) mimic the EDM signal and these will require more study [11,13,14]. The expected systematic uncertainty of the Mott polarimeter is $\delta P \approx 1$ μ rad, similar to the EDM polarimeter at COSY [43].

9. Dark energy and ultra-light dark matter search

As in the ME based design, the low energy ST storage ring can also be used to search for spin precession induced by dark energy and ultra-light (axion) dark matter (DE/DM). The axion field gradient couples to the spin of transversely polarized electrons stored in the ring with a sensitivity proportional to the relativistic beam velocity, β, and SCT [44]. Since the proposed ST ring has a small size, one ring can be used to store longitudinally polarized electrons to measure EDM while a second ring can be used to store transversely polarized electrons for DE/DM search. Unlike the EDM ring, for the DE/DM ring, one can use an identical ring to EDM, or Figure-8 electric ring without longitudinal electric fields. For this search, the spin rotates around the electron's velocity and the main systematic uncertainty is longitudinal background magnetic field that rotates the spin of the CRA and CRB beams in the same direction. However, DE/DM interaction will rotate the spin in opposite directions, resulting in cancellation of this background effect when combining CRA and CRB data.

Another method to probe dark matter is to measure oscillation in the EDM signal in the presence of an axion field [41,45,46].

10. ST concept developments in progress

A similar ring to the one discussed above can be used to measure the positron EDM. Generating and accumulating polarized positron bunches have been extensively studied in relation to other projects [47] and was found to be very achievable. The ST ring concept could potentially be extended to low-energy polarized proton, deuteron, and muon beams using rings of comparable dimensions to those described here for electrons, although for this all-electric design, it is harder to create a substantial difference in γ for heavy particles. At a minimum, the all-electric, two-energy design presented here can serve as a testbed for EDM searches of these other particles. Also, one may consider a low-energy ST ring based on an electro-magnetic design [16]. The advantages of accessibility, low cost, and simplicity of beam and polarization control and diagnostics might outweigh the disadvantage of the absence of a CR beam.

Techniques of compensation and control for spin coherent and decoherent detunes due to background magnetic fields, imperfections, and beam emittances are under consideration by several collaborations. In particular, an intriguing possibility of implementing the Spin Echo technique [48] in low-energy rings with bunched beams is under study [16].

11. Summary

We described a new method to directly measure d_e to projected statistical limit of about 5.8×10^{-30} $e \cdot$cm and to search for DE/DM using small ST rings in the energy range below 1 MeV. The presented approach has the following advantages: CR beams, energy-independent spin tune, long SCT, bunched beam, any energy, spin-achromatic beam transport, no synchrotron radiation, minimum safety issues, straightforward polarimetry, room-sized facility, good control of systematic effects and imperfections including background magnetic fields, manageable, low cost, and finally, such rings can serve as testbed for larger-scale experiments.

Declaration of competing interest

The authors declare that they have no known competing financial interests or personal relationships that could have appeared to influence the work reported in this paper.

Data availability

Data will be made available on request.

Acknowledgements

We appreciate very helpful discussions with M. Blaskiewicz, A. Hutton, Yu. N. Filatov, A. M. Kondratenko, M. A. Kondratenko, V. Lebedev, R. Li, M. Poelker, and T. Satogata. This material is based upon work supported by the U.S. Department of Energy, Office of Science, Office of Nuclear Physics under contract DE-AC05-06OR23177. This manuscript has been authored in part by UT-Battelle, LLC, under contract DE-AC05-00OR22725 with the US Department of Energy (DOE). The publisher acknowledges the US government license to provide public access under the DOE Public Access Plan (http://energy.gov/downloads/doe-public-access-plan).

References

[1] T.E. Chupp, P. Fierlinger, M.J. Ramsey-Musolf, J.T. Singh, Electric dipole moments of atoms, molecules, nuclei, and particles, Rev. Mod. Phys. 91 (2019) 015001, https://doi.org/10.1103/RevModPhys.91.015001, https://link.aps.org/doi/10.1103/RevModPhys.91.015001.

[2] N. Fortson, P. Sandars, S. Barr, The Search for a Permanent Electric Dipole Moment, Phys. Today 56 (2003) 33, https://doi.org/10.1063/1.1595052.

[3] N. Yamanaka, Review of the electric dipole moment of light nuclei, Int. J. Mod. Phys. E 26 (2017) 1730002, https://doi.org/10.1142/S0218301317300028.

[4] T.S. Roussy, L. Caldwell, T. Wright, W.B. Cairncross, Y. Shagam, K.B. Ng, N. Schlossberger, S.Y. Park, A. Wang, J. Ye, E.A. Cornell, A new bound on the electron's electric dipole moment, arXiv:2212.11841, 2022, https://doi.org/10.48550/arXiv.2212.11841.

[5] B. Graner, Y. Chen, E.G. Lindahl, B.R. Heckel, Reduced Limit on the Permanent Electric Dipole Moment of ^{199}Hg, Phys. Rev. Lett. 116 (2016) 161601, https://doi.org/10.1103/PhysRevLett.116.161601, https://link.aps.org/doi/10.1103/PhysRevLett.116.161601.

[6] C. Abel, S. Afach, N.J. Ayres, C.A. Baker, G. Ban, G. Bison, K. Bodek, V. Bondar, M. Burghoff, E. Chanel, Z. Chowdhuri, P.-J. Chiu, B. Clement, C.B. Crawford, M. Daum, S. Emmenegger, L. Ferraris-Bouchez, M. Fertl, P. Flaux, B. Franke, A. Fratangelo, P. Geltenbort, K. Green, W.C. Griffith, M. van der Grinten, Z.D. Grujić, P.G. Harris, L. Hayen, W. Heil, R. Henneck, V. Hélaine, N. Hild, Z. Hodge, M. Horras, P. Iaydjiev, S.N. Ivanov, M. Kasprzak, Y. Kermaidic, K. Kirch, A. Knecht, P. Knowles, H.-C. Koch, P.A. Koss, S. Komposch, A. Kozela, A. Kraft, J. Krempel, M. Kuźniak, B. Lauss, T. Lefort, Y. Lemière, A. Leredde, P. Mohanmurthy, A. Mtchedlishvili, M. Musgrave, O. Naviliat-Cuncic, D. Pais, F.M. Piegsa, E. Pierre, G. Pignol, C. Plonka-Spehr, P.N. Prashanth, G. Quéméner, M. Rawlik, D. Rebreyend, I. Rienäcker, D. Ries, S. Roccia, G. Rogel, D. Rozpedzik, A. Schnabel, P. Schmidt-Wellenburg, N. Severijns, D. Shiers, R. Tavakoli Dinani, J.A. Thorne, R. Virot, J. Voigt, A. Weis, E. Wursten, G. Wyszynski, J. Zejma, J. Zenner, G. Zsigmond, Measurement of the Permanent Electric Dipole Moment of the Neutron, Phys. Rev. Lett. 124 (2020) 081803, https://doi.org/10.1103/PhysRevLett.124.081803, https://link.aps.org/doi/10.1103/PhysRevLett.124.081803.

[7] G.W. Bennett, B. Bousquet, H.N. Brown, G. Bunce, R.M. Carey, P. Cushman, G.T. Danby, P.T. Debevec, M. Deile, H. Deng, W. Deninger, S.K. Dhawan, V.P. Druzhinin, L. Duong, E. Efstathiadis, F.J.M. Farley, G.V. Fedotovich, S. Giron, F.E. Gray, D. Grigoriev, M. Grosse-Perdekamp, A. Grossmann, M.F. Hare, D.W. Hertzog, X. Huang, V.W. Hughes, M. Iwasaki, K. Jungmann, D. Kawall, M. Kawamura, B.I. Khazin, J. Kindem, F. Krienen, I. Kronkvist, A. Lam, R. Larsen, Y.Y. Lee, I. Logashenko, R. McNabb, W. Meng, J. Mi, J.P. Miller, Y. Mizumachi, W.M. Morse, D. Nikas, C.J.G. Onderwater, Y. Orlov, C.S. Özben, J.M. Paley, Q. Peng, C.C. Polly, J. Pretz, R. Prigl, G. zu Putlitz, T. Qian, S.I. Redin, O. Rind, B.L. Roberts, N. Ryskulov, S. Sedykh, Y.K. Semertzidis, P. Shagin, Y.M. Shatunov, E.P. Sichtermann, E. Solodov, M. Sossong, A. Steinmetz, L.R. Sulak, C. Timmermans, A. Trofimov, D. Urner, P. von Walter, D. Warburton, D. Winn, A. Yamamoto, D. Zimmerman, Muon ($g-2$) Collaboration, Improved limit on the muon electric dipole moment, Phys. Rev. D 80 (2009) 052008, https://doi.org/10.1103/PhysRevD.80.052008, https://link.aps.org/doi/10.1103/PhysRevD.80.052008.

[8] T. Fukuyama, A.J. Silenko, Derivation of Generalized Thomas-Bargmann-Michel-Telegdi Equation for a Particle with Electric Dipole Moment, International Journal of Modern Physics A 28 (2013) 1350147, https://doi.org/10.1142/S0217751X13501479.

[9] F.J.M. Farley, K. Jungmann, J.P. Miller, W.M. Morse, Y.F. Orlov, B.L. Roberts, Y.K. Semertzidis, A. Silenko, E.J. Stephenson, New Method of Measuring Electric Dipole Moments in Storage Rings, Phys. Rev. Lett. 93 (2004) 052001, https://doi.org/10.1103/PhysRevLett.93.052001, https://link.aps.org/doi/10.1103/PhysRevLett.93.052001.

[10] V. Anastassopoulos, et al., Storage Ring EDM Collaboration, A proposal to measure the proton electric dipole moment with 10^{-29} $e \cdot$cm sensitivity, http://www.bnl.gov/edm, 2011.

[11] F. Abusaif, A. Aggarwal, A. Aksentev, B. Alberdi-Esuain, A. Atanasov, L. Barion, S. Basile, M. Berz, M. Beyß, C. Böhme, J. Böker, J. Borburgh, C. Carli, I. Ciepał, G. Ciullo, M. Contalbrigo, J.M.D. Conto, S. Dymov, O. Felden, M. Gagoshidze,

M. Gaisser, R. Gebel, N. Giese, K. Grigoryev, D. Grzonka, M.H. Tahar, T. Hahnraths, D. Heberling, V. Hejny, J. Hetzel, D. Hölscher, O. Javakhishvili, L. Jorat, A. Kacharava, V. Kamerdzhiev, S. Karanth, C. Käseberg, I. Keshelashvili, I. Koop, A. Kulikov, K. Laihem, M. Lamont, A. Lehrach, P. Lenisa, N. Lomidze, B. Lorentz, G. Macharashvili, A. Magiera, K. Makino, S. Martin, D. Mchedlishvili, U.G. Meißner, Z. Metreveli, J. Michaud, F. Müller, A. Nass, G. Natour, N. Nikolaev, A. Nogga, A. Pesce, V. Poncza, D. Prasuhn, J. Pretz, F. Rathmann, J. Ritman, M. Rosenthal, A. Saleev, M. Schott, T. Sefzick, Y. Senichev, D. Shergelashvili, V. Shmakova, S. Siddique, A. Silenko, M. Simon, J. Slim, H. Soltner, A. Stahl, R. Stassen, E. Stephenson, H. Straatmann, H. Ströher, M. Tabidze, G. Tagliente, R. Talman, Y. Uzikov, Y. Valdau, E. Valetov, T. Wagner, C. Weidemann, A. Wirzba, A. Wrońska, P. Wüstner, P. Zupranski, M. Żurek, Storage Ring to Search for Electric Dipole Moments of Charged Particles – Feasibility Study, arXiv:1912.07881, 2019, https://doi.org/10.48550/arXiv.1912.07881.

[12] V. Anastassopoulos, S. Andrianov, R. Baartman, S. Baessler, M. Bai, J. Benante, M. Berz, M. Blaskiewicz, T. Bowcock, K. Brown, B. Casey, M. Conte, J.D. Crnkovic, N. D'Imperio, G. Fanourakis, A. Fedotov, P. Fierlinger, W. Fischer, M.O. Gaisser, Y. Giomataris, M. Grosse-Perdekamp, G. Guidoboni, S. Hacıömeroğlu, G. Hoffstaetter, H. Huang, M. Incagli, A. Ivanov, D. Kawall, Y.I. Kim, B. King, I.A. Koop, D.M. Lazarus, V. Lebedev, M.J. Lee, S. Lee, Y.H. Lee, A. Lehrach, P. Lenisa, P. Levi Sandri, A.U. Luccio, A. Lyapin, W. MacKay, R. Maier, K. Makino, N. Malitsky, W.J. Marciano, W. Meng, F. Meot, E.M. Metodiev, L. Miceli, D. Moricciani, W.M. Morse, S. Nagaitsev, S.K. Nayak, Y.F. Orlov, C.S. Ozben, S.T. Park, A. Pesce, E. Petrakou, P. Pile, B. Podobedov, V. Polychronakos, J. Pretz, V. Ptitsyn, E. Ramberg, D. Raparia, F. Rathmann, S. Rescia, T. Roser, H. Kamal Sayed, Y.K. Semertzidis, Y. Senichev, A. Sidorin, A. Silenko, N. Simos, A. Stahl, E.J. Stephenson, H. Ströher, M.J. Syphers, J. Talman, R.M. Talman, V. Tishchenko, C. Touramanis, N. Tsoupas, G. Venanzoni, K. Vetter, S. Vlassis, E. Won, G. Zavattini, A. Zelenski, K. Zioutas, A storage ring experiment to detect a proton electric dipole moment, Rev. Sci. Instrum. 87 (2016) 115116, https://doi.org/10.1063/1.4967465.

[13] S. Hacıömeroğlu, Y.K. Semertzidis, Hybrid ring design in the storage-ring proton electric dipole moment experiment, Phys. Rev. Accel. Beams 22 (2019) 034001, https://doi.org/10.1103/PhysRevAccelBeams.22.034001, https://link.aps.org/doi/10.1103/PhysRevAccelBeams.22.034001.

[14] Z. Omarov, H. Davoudiasl, S. Hacıömeroğlu, V. Lebedev, W.M. Morse, Y.K. Semertzidis, A.J. Silenko, E.J. Stephenson, R. Suleiman, Comprehensive symmetric-hybrid ring design for a proton EDM experiment at below 10^{-29} e · cm, Phys. Rev. D 105 (2022) 032001, https://doi.org/10.1103/PhysRevD.105.032001, https://link.aps.org/doi/10.1103/PhysRevD.105.032001.

[15] G. Guidoboni, E. Stephenson, S. Andrianov, W. Augustyniak, Z. Bagdasarian, M. Bai, M. Baylac, W. Bernreuther, S. Bertelli, M. Berz, J. Böker, C. Böhme, J. Bsaisou, S. Chekmenev, D. Chiladze, G. Ciullo, M. Contalbrigo, J.-M. de Conto, S. Dymov, R. Engels, F.M. Esser, D. Eversmann, O. Felden, M. Gaisser, R. Gebel, H. Glückler, F. Goldenbaum, K. Grigoryev, D. Grzonka, T. Hahnraths, D. Heberling, V. Hejny, N. Hempelmann, J. Hetzel, F. Hinder, R. Hipple, D. Hölscher, A. Ivanov, A. Kacharava, V. Kamerdzhiev, B. Kamys, I. Keshelashvili, A. Khoukaz, I. Koop, H.-J. Krause, S. Krewald, A. Kulikov, A. Lehrach, P. Lenisa, N. Lomidze, B. Lorentz, P. Maanen, G. Macharashvili, A. Magiera, R. Maier, K. Makino, B. Mariański, D. Mchedlishvili, U.-G. Meißner, S. Mey, W. Morse, F. Müller, A. Nass, G. Natour, N. Nikolaev, M. Nioradze, K. Nowakowski, Y. Orlov, A. Pesce, D. Prasuhn, J. Pretz, F. Rathmann, J. Ritman, M. Rosenthal, Z. Rudy, A. Saleev, T. Sefzick, Y. Semertzidis, Y. Senichev, V. Shmakova, A. Silenko, M. Simon, J. Slim, H. Soltner, A. Stahl, R. Stassen, M. Statera, H. Stockhorst, H. Straatmann, H. Ströher, M. Tabidze, R. Talman, P. Thörngren Engblom, F. Trinkel, A. Trzciński, Y. Uzikov, Y. Valdau, E. Valetov, A. Vassiliev, C. Weidemann, C. Wilkin, A. Wrońska, P. Wüstner, M. Zakrzewska, P. Zuprański, D. Zyuzin, JEDI Collaboration, How to Reach a Thousand-Second in-Plane Polarization Lifetime with 0.97-GeV/c Deuterons in a Storage Ring, Phys. Rev. Lett. 117 (2016) 054801, https://doi.org/10.1103/PhysRevLett.117.054801, https://link.aps.org/doi/10.1103/PhysRevLett.117.054801.

[16] R. Suleiman, V.S. Morozov, Y.S. Derbenev, On Possibilities of High Precision Experiments in Fundamental Physics in Storage Rings of Low Energy Polarized Electron Beams, arXiv:2105.11575, 2021, https://doi.org/10.48550/arXiv.2105.11575.

[17] Y.N. Filatov, A.M. Kondratenko, M.A. Kondratenko, Y.S. Derbenev, V.S. Morozov, Transparent Spin Method for Spin Control of Hadron Beams in Colliders, Phys. Rev. Lett. 124 (2020) 194801, https://doi.org/10.1103/PhysRevLett.124.194801, https://link.aps.org/doi/10.1103/PhysRevLett.124.194801.

[18] A. Kondratenko, M. Kondratenko, Y. Filatov, A. Kovalenko, Y. Derbenev, V. Morozov, Feasibility of measuring EDM in spin transparent colliders, EPJ Web Conf. 204 (2019) 10013, https://doi.org/10.1051/epjconf/201920410013.

[19] J. Flanz, C. Sargent, Operation of an isochronous beam recirculation system, Nucl. Instrum. Methods Phys. Res., Sect. A, Accel. Spectrom. Detect. Assoc. Equip. 241 (1985) 325–333, https://doi.org/10.1016/0168-9002(85)90585-6, https://www.sciencedirect.com/science/article/pii/0168900285905856.

[20] M. Conte, M. Martini, Intrabeam Scattering in the CERN Anti-Proton Accumulator, Part. Accel. 17 (1985) 1–10, http://cdsweb.cern.ch/record/457572/files/p1.pdf.

[21] MAD-X, Methodical accelerator design, http://mad.web.cern.ch/mad, 2022.

[22] J. Marriner, Stochastic cooling overview, in: International Workshop on Beam Cooling and Related Topics, Nucl. Instrum. Methods Phys. Res., Sect. A, Accel. Spectrom. Detect. Assoc. Equip. 532 (2004) 11–18, https://doi.org/10.1016/j.nima.2004.06.025, https://www.sciencedirect.com/science/article/pii/S0168900204011507.

[23] D. Möhl, Stochastic Cooling for Beginners, in: Conf. Proc. C 831011, 1983, pp. 97–161, https://inspirehep.net/files/bdfebe85390380a11e2f80e27621d81f.

[24] S.Y. Lee, Accelerator Physics, Fourth Edition, World Scientific Publishing Company, 2018, https://doi.org/10.1142/11111.

[25] J. Eldred, V. Lebedev, K. Seiya, V. Shiltsev, Beam intensity effects in Fermilab Booster synchrotron, Phys. Rev. Accel. Beams 24 (2021) 044001, https://doi.org/10.1103/PhysRevAccelBeams.24.044001, https://link.aps.org/doi/10.1103/PhysRevAccelBeams.24.044001.

[26] R.A. Kishek, G. Bai, B. Beaudoin, S. Bernal, D. Feldman, R. Feldman, R. Fiorito, T. Godlove, I. Haber, T. Langford, P. O'Shea, B. Quinn, C. Papadopoulos, M. Reiser, D. Stratakis, D. Sutter, K. Tian, J. Thangaraj, M. Walter, C. Wu, The University of Maryland Electron Ring (UMER) enters a new regime of high-tune-shift rings, in: 2007 IEEE Particle Accelerator Conference (PAC), 2007, pp. 820–824, https://doi.org/10.1109/PAC.2007.4441116.

[27] J.B. Murphy, S. Krinsky, R.L. Gluckstern, Longitudinal wake field for an electron moving on a circular orbit, Part. Accel. 57 (1997) 9–64, https://inspirehep.net/files/1afd5dcc4e791d233fb0ffb5a2f270a4.

[28] R. Warnock, P.M. Morton, Fields excited by a beam in a smooth toroidal chamber, Part. Accel. 25 (1990) 113–151, http://slac.stanford.edu/pubs/slacpubs/4500/slac-pub-4562.pdf.

[29] M.L. Stutzman, P.A. Adderley, M.A.A. Mamun, M. Poelker, Nonevaporable getter coating chambers for extreme high vacuum, J. Vac. Sci. Technol. A 36 (2018) 031603, https://doi.org/10.1116/1.5010154.

[30] Y.N. Filatov, A.M. Kondratenko, M.A. Kondratenko, Y.S. Derbenev, V.S. Morozov, A.D. Kovalenko, Spin response function technique in spin-transparent synchrotrons, Eur. Phys. J. C 80 (2020) 778, https://doi.org/10.1140/epjc/s10052-020-8344-5.

[31] A.M. Kondratenko, M.A. Kondratenko, Y.N. Filatov, Y.S. Derbenev, F. Lin, V.S. Morozov, Y. Zhang, Acceleration of polarized protons and deuterons in the ion collider ring of JLEIC, J. Phys. Conf. Ser. 874 (2017) 012011, https://doi.org/10.1088/1742-6596/874/1/012011.

[32] P.A. Adderley, J. Clark, J. Grames, J. Hansknecht, K. Surles-Law, D. Machie, M. Poelker, M.L. Stutzman, R. Suleiman, Load-locked dc high voltage GaAs photogun with an inverted-geometry ceramic insulator, Phys. Rev. Spec. Top., Accel. Beams 13 (2010) 010101, https://doi.org/10.1103/PhysRevSTAB.13.010101, https://link.aps.org/doi/10.1103/PhysRevSTAB.13.010101.

[33] J. Grames, P. Adderley, J. Benesch, J. Clark, J. Hansknecht, R. Kazimi, D. Machie, M. Poelker, M. Stutzman, R. Suleiman, Y. Zhang, Two Wien Filter Spin Flipper, in: Proceedings of 2011 Particle Accelerator Conference, New York, NY, USA, 2011, pp. 862–864, https://accelconf.web.cern.ch/pac2011/papers/tup025.pdf.

[34] P. Adderley, D. Bullard, Y. Chao, C. Garcia, J. Grames, J. Hansknecht, A. Hofler, R. Kazimi, J. Musson, C. Palatchi, K. Paschke, M. Poelker, G. Smith, M. Stutzman, R. Suleiman, Y. Wang, An overview of how parity-violating electron scattering experiments are performed at CEBAF, Nucl. Instrum. Methods Phys. Res., Sect. A, Accel. Spectrom. Detect. Assoc. Equip. 1046 (2023) 167710, https://doi.org/10.1016/j.nima.2022.167710, https://www.sciencedirect.com/science/article/pii/S0168900222010026.

[35] T.J. Gay, F.B. Dunning, Mott electron polarimetry, Rev. Sci. Instrum. 63 (1992) 1635–1651, https://doi.org/10.1063/1.1143371.

[36] V. Tioukine, K. Aulenbacher, E. Riehn, A Mott polarimeter operating at MeV electron beam energies, Rev. Sci. Instrum. 82 (2011) 033303, https://doi.org/10.1063/1.3556593.

[37] K. Aulenbacher, E. Chudakov, D. Gaskell, J. Grames, K.D. Paschke, Precision electron beam polarimetry for next generation nuclear physics experiments, Int. J. Mod. Phys. E 27 (2018) 1830004, https://doi.org/10.1142/S0218301318300047.

[38] J.M. Grames, C.K. Sinclair, M. Poelker, X. Roca-Maza, M.L. Stutzman, R. Suleiman, M.A. Mamun, M. McHugh, D. Moser, J. Hansknecht, B. Moffit, T.J. Gay, High precision 5 MeV Mott polarimeter, Phys. Rev. C 102 (2020) 015501, https://doi.org/10.1103/PhysRevC.102.015501, https://link.aps.org/doi/10.1103/PhysRevC.102.015501.

[39] X. Roca-Maza, Theoretical calculations for precision polarimetry based on Mott scattering, Europhys. Lett. 120 (2017) 33002, https://doi.org/10.1209/0295-5075/120/33002.

[40] X. Roca-Maza, 2021, private communication.

[41] O. Kim, Y.K. Semertzidis, New method of probing an oscillating EDM induced by axionlike dark matter using an rf Wien filter in storage rings, Phys. Rev. D 104 (2021) 096006, https://doi.org/10.1103/PhysRevD.104.096006, https://link.aps.org/doi/10.1103/PhysRevD.104.096006.

[42] C. Carli, M. Haj Tahar, Geometric phase effect study in electric dipole moment rings, Phys. Rev. Accel. Beams 25 (2022) 064001, https://doi.org/10.1103/PhysRevAccelBeams.25.064001, https://link.aps.org/doi/10.1103/PhysRevAccelBeams.25.064001.

[43] N.P.M. Brantjes, V. Dzordzhadze, R. Gebel, F. Gonnella, F. Gray, D. van der Hoek, A. Imig, W. Kruithof, D. Lazarus, A. Lehrach, B. Lorentz, R. Messi, D. Moricciani, W. Morse, G. Noid, C. Onderwater, C. Özben, D. Prasuhn, P. Levi Sandri,

Y. Semertzidis, M. da Silva e Silva, E. Stephenson, H. Stockhorst, G. Venanzoni, O. Versolato, Correcting systematic errors in high-sensitivity deuteron polarization measurements, Nucl. Instrum. Methods Phys. Res., Sect. A, Accel. Spectrom. Detect. Assoc. Equip. 664 (2012) 49–64, https://doi.org/10.1016/j.nima.2011.09.055, https://www.sciencedirect.com/science/article/pii/S016890021101850X.

[44] P.W. Graham, S. Hacıömeroğlu, D.E. Kaplan, Z. Omarov, S. Rajendran, Y.K. Semertzidis, Storage ring probes of dark matter and dark energy, Phys. Rev. D 103 (2021) 055010, https://doi.org/10.1103/PhysRevD.103.055010, https://link.aps.org/doi/10.1103/PhysRevD.103.055010.

[45] S.P. Chang, S. Hacıömeroğlu, O. Kim, S. Lee, S. Park, Y.K. Semertzidis, Axionlike dark matter search using the storage ring EDM method, Phys. Rev. D 99 (2019) 083002, https://doi.org/10.1103/PhysRevD.99.083002, https://link.aps.org/doi/10.1103/PhysRevD.99.083002.

[46] J. Pretz, S.P. Chang, V. Hejny, S. Karanth, S. Park, Y. Semertzidis, E. Stephenson, H. Ströher, Statistical sensitivity estimates for oscillating electric dipole moment measurements in storage rings, Eur. Phys. J. C 80 (2020) 107, https://doi.org/10.1140/epjc/s10052-020-7664-9.

[47] F. Lin, J. Grames, J. Guo, V. Morozov, Y. Zhang, Polarized positrons in Jefferson Lab Electron-Ion Collider (JLEIC), AIP Conf. Proc. (2018) 1970, https://doi.org/10.1063/1.5040224, p. 050005.

[48] Y.S. Derbenev, Y.N. Filatov, A.M. Kondratenko, M.A. Kondratenko, V.S. Morozov, Siberian Snakes, Figure-8 and Spin Transparency Techniques for High Precision Experiments with Polarized Hadron Beams in Colliders, Symmetry 13 (2021) 398, https://doi.org/10.3390/sym13030398, https://www.mdpi.com/2073-8994/13/3/398.